J. For. Res. 5: 247–258 (2000)

Stand Parameter Estimation of Artificial Evergreen Conifer Forests Using Airborne Images: An Evaluation of Seasonal Difference on Accuracy and Best Wavelength

Yoshio Awaya,*1,[1] Nobuhiko Tanaka,*2 Kunihiro Tanaka,*1 Gen Takao,*3 Eiji Kodani,*4 and Satoshi Tsuyuki*5

*1 Tohoku Research Center, Forestry and Forest Products Research Institute, Morioka 020–0123, Japan.
*2 Forestry and Forest Products Research Institute, Ibaraki 305–8687, Japan.
*3 Hokkaido Research Center, Forestry and Forest Products Research Institute, Sapporo 062–0045, Japan.
*4 Shikoku Research Center, Forestry and Forest Products Research Institute, Kochi 780–8064, Japan.
*5 Graduate School of Agricultural and Life Sciences, The University of Tokyo, Tokyo 113–8657, Japan.

The relationship between the stand parameters (top layer height (H1) and volume/ha (Vha)) and digital number (DN) were evaluated for evergreen conifer stands using three airborne images with 4-m spatial resolution, which were taken in June 1995, September 1993, and October 1994 using the Compact Airborne Spectrographic Imager (CASI). Estimation accuracy of the stand parameters, their seasonal changes, and suitable wavelength were analyzed using correlation coefficients and a regression analysis. The minimum DN of stands, which showed the darkness of a canopy shadow, had a higher correlation with H1 than the average and maximum DN while the average DN had a higher correlation with Vha. The green channels gave the highest correlation coefficients with H1 and Vha, which exceeded − 0.9 for the September and October images. However, the red channels had a consistently high correlation with the stand parameters for the three images. The near infrared channels gave poor correlations with H1 and Vha for the June image. Spectral variations among trees may affect the relationship between DN and the stand parameters in the leaf maturation period in June. Consequently, the late growing season was better at giving consistent results for the stand parameter studies. There was a linear relationship between the measured and the estimated stand parameters for the validation plots especially for the H1 case of September with sufficient accuracy. Nadir viewing images, which had high spatial resolution and a wide dynamic range such as the CASI images, were necessary to estimate the stand parameters accurately.

Key words: CASI, conifer, remote sensing, seasonal change, stand parameter

Standing volume is not only one of the most important parameters in forest management, but also one of the major political interests after the 3rd Session of the Conference of the Parties to United Nations Framework Convention on Climate Change (COP3) in 1997. If stem volume and other stand parameters are estimated in large areas with sufficient accuracy, they can be used for forest management to replace or supplement the current inventory system. Such spatial information may also be important in political decision making. Remotely sensed data have potential for above accurate biomass estimation, which has been one of the common interests for many researchers since the launch of Landsat 1.

The Thematic Mapper (TM) of Landsat has been the most popular space-borne sensor for the last decade. The TM records the brightness of ground objects in 256 gray levels. Sixteen detectors in each reflective channel cause stripes, which are output levels altered by the detectors within a few gray levels, due to improper calibration of the detectors especially in the visible channels in forests. Although the TM digitizes objects in 256 gray levels, the data ranges of dense evergreen conifer stands are usually less than 10 in digital number (DN) in visible channels, and only about 2 or 3 in the red channel. The stripes degrade signals in visible channels greatly in dense conifer stands. Thus the narrow dynamic range and poor signal-to-noise ratio of space-borne sensors may affect the accuracy of the forest analysis. On the other hand, with advances in technology, airborne optical sensors have been improved drastically during the last decade. Hyperspectral channels with narrower spectral ranges are achieved, and wider dynamic ranges and better signal-to-noise ratio make it possible to identify slight radiation differences in targets. The Compact Airborne Spectrographic Imager (CASI) (Babey and Anger, 1989) is one of these airborne sensors. The observation parameters of the CASI can be programmed by the operator and it observes in the visible and near infrared (NIR) regions with a minimum of 1.8-nm spectral resolution. Images used in this study have 15 or 16 channels with 30-nm spectral resolution, 4-m spatial resolution and a 12-bit dynamic range. The specifications of CASI images are superior to those of satellite sensor images, and these specifications would not be a limiting factor for forest analysis. The technology will be applied to space-borne sensors in the near future. Thus, there is a great possibility to improve the accuracy of stand parameter estimation in large areas without the limitation of sensor performance.

With agricultural crops there is a curvilinear relationship between the leaf area index (LAI) and radiance or reflectance factors (Holben *et al.*, 1980; Curran, 1983; Huete, 1987). Such a relationship is simulated by radiative transfer models of canopy (*e.g.*, Sellers, 1987). As in crops, the relationship between LAI of forests and satellite sensor signals, namely radiance, has been studied previously (Peterson *et al.*, 1987; Curran *et al.*, 1990; Spanner *et al.*, 1990; Baulies and Pons, 1995; Chen and Cihlar, 1996). On the other hand, some

[1] Corresponding author.

models show that stand structures such as canopy coverage, canopy size, and canopy shadow have influences on reflectance or radiance (Strahler *et al.*, 1988; Nilson and Peterson, 1994), and the parameters are computed from satellite data by an inversion of the model (*e.g.*, Strahler *et al.*, 1988). Thus, it is reasonable to study stand parameters such as diameter at breast height (DBH), tree height, and stem volume using remote sensing data. Actually, several studies have estimated these parameters using high spatial resolution data (Franklin, 1986; Cohen and Spies, 1992; Franklin and McDermid, 1993; Baulies and Pons, 1995; Cohen *et al.*, 1995; Gemmell, 1995; Trotter *et al.*, 1997). Textural features of images are also important entities in stand attribute studies, especially for very high spatial resolution data taken from airplanes (Cohen *et al.*, 1990; Cohen and Spies, 1992; Franklin and McDermid, 1993; St-Onge and Cavayas, 1997). The stand parameters can be estimated well by using radiance data for the boreal and temperate coniferous forests (Franklin, 1986; Cohen and Spies, 1992; Franklin and McDermid, 1993; Baulies and Pons, 1995; Cohen *et al.*, 1995; Trotter *et al.*, 1997). However, seasonal and species differences are not understood. Seasonal variations of vegetation spectra (Blackburn and Milton, 1995; Awaya and Tanaka, 1999) and differences of spectra among trees and/or species probably reduce the accuracy of stand parameter estimations.

Topography (Leprieur *et al.*, 1988) and forest floor spectra (Spanner *et al.*, 1990; Awaya *et al.*, 1992) also influence the spectra of stands. DN varies greatly with slope and aspect, and the topographic influence on DN is much greater than the influence of biomass or tree size in steep terrain. Meanwhile, the relationships between LAI and DN in the NIR and the intensity of a vegetation index are also changed significantly by canopy closure, and affected by the undergrowth in open canopy forests (Spanner *et al.*, 1990). When the canopy closure is small, the radiance changes with the change of the closure due to the influence of forest floor (Awaya *et al.*, 1992). As a result, the spectra of forest floors interfere with the biomass analysis when the canopy is not closed sufficiently. Since this paper focuses on the evaluation of relationships between DN and the stand parameters and their seasonal differences, it was necessary to avoid the influences of topography and the forest floor. Therefore, closed forests on flat terrain were selected in this study to examine relationships that are free from the effects of topography and forest floor.

This study aims to make an accurate stand parameter estimation by using airborne images, which have sufficient data ranges, and fine spatial and spectral resolutions. Here we discuss (1) the relationship between the stand parameters and radiance data of airborne images in evergreen conifer stands, (2) the best season for estimation of the stand parameters, (3) the best wavelength channel for estimation of the stand parameters, and (4) the accuracy of the estimated stand parameters using the images.

Study Site and Data

1 Study site

The study site was situated in the national forest near Tomakomai, Hokkaido, Japan (Fig. 1, 42° 45′ N, 141° 32′ E). It had a very flat topography with an elevation of approximately 100 m above sea level, and was located in the transition zone between the cool temperate forest and boreal forest. Most of the forests in this area were artificial plantations of Ezo spruce (*Picea jezoenthis* Carr.), Akaezo spruce (*Picea glehnii* Mast.), Todo fir (*Abies sachalinensis* var. *mayriana* Miyabe et Kudo), Japanese larch (*Larix kaempferi* Carr.), *etc.* We classified forest plantations into 4 groups according to the plantation history. They were, Ezo spruce planted before 1945 (Group 1), Ezo spruce planted between 1945 and 1955 (Group 2), Japanese larch planted between 1955 and the early 1960s (Group 3), and Akaezo spruce, Ezo spruce and Todo fir planted since the mid 1960s (Group 4) (Tomakomai Forestry Office, 1993). Although Ezo spruce was the main planted species, most stands were mixed forests with Ezo spruce and Todo fir in Group 1. There were few plantations in Group 2. As large forests had been damaged seriously by a typhoon in 1954, broad-leaved trees started to grow in conifer plantations after the damage and many damaged areas were also replanted. Considering such a plantation history and forest conditions, spruce-dominated stands were mainly selected in Groups 1 and 4 with 3 fir stands in Group 4 for the study.

2 Field surveys

Field surveys were conducted four times (July 19 to 23, 1993, September 9 to 13, 1994, June 6 to 10, 1995, and July 22 to 26, 1997). The plot area was between 0.01 and 0.09 ha and was chosen according to tree height. The DBH was measured for all trees greater than or equal to 4 cm, and tree height was measured for three trees in the top layer, one tree

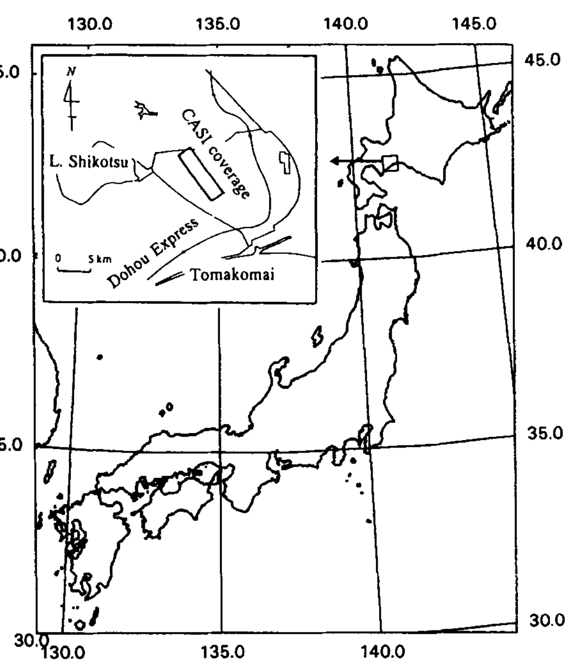

Fig. 1 Location of study site.

in the middle layer and one tree in the lower layer in each plot. The plot location was measured using a compass and tape measure from any clear point on maps or aerial photos. Only the plots with clear location documentation were used in the analysis.

3 Airborne data

A Canadian airborne sensor, the CASI of Iters Research Ltd., was used to collect remote sensing data. The CASI was able to measure spectral radiation from 420 to 920 nm. The spectral positions of the channels could be set freely to 18 channels for the spectral mode on condition that these channels did not overlap each other. Several flights were executed in three different seasons by the National Space Development Agency of Japan (NASDA). The specifications of CASI and the images, which were used in the analysis, are shown in Table 1. A part of the images, which covered 8 km by 2 km approximately, was used in this study (Fig. 1). Geometric skews of the images, which were caused by unstable airplane positions, were corrected as much as possible by the system software of Iters Research Ltd. Although CASI data were converted to radiance values, the term DN is still used in this paper due to uncertainty of the sensor calibration. DN showed a linear relationship with radiance values, and hence showed a linear relationship with reflectance factors on flat terrain for all channels.

4 Reference data

Black and white aerial photos of 1: 20,000 and 1: 24,000, which were taken in 1990 and 1991 by the Forestry Agency and the Geographical Survey Institute of Japan, respectively, were used to check stand conditions. Color aerial photos 1: 20,000, which were taken on August 2, 1993 by NASDA using a Hasselblad camera, were also used. Plot locations were marked on the color aerial photos according to the forest planning maps 1: 20,000 of Tomakomai and Eniwa forestry offices and the location documents.

Methods

1 Plot data compilation

Two tree height-diameter curves were exploited to estimate tree height, one for conifer trees (Eq. (1)) and the other for broad-leaved trees (Eq. (2), Nakashima, 1946).

$$H = DBH^2 / (2.709 + 0.1621 \cdot DBH)^2 + 1.3 \quad (1)$$

$$H = 0.67474 \cdot DBH^{1.44326} \cdot 0.74271^{\sqrt{DBH}} + 1.3 \quad (2)$$

where *DBH* was the diameter at breast height and H was the tree height.

The first equation was derived from the DBH and height of 150 trees measured in 1993. The tree height was calculated using the curves for each tree in all plots. Stem volume was estimated for each tree using the measured DBH, the calculated height and stem volume equations for spruce, fir and broad-leaves (Hokkaido Forestry Bureau, 1970). Four different groups of trees were considered in each plot. The average height of the highest 10% of the trees in each plot (Htop) was calculated. Groups T1, T2, and T3 consisted of trees whose heights were at least three fourths, one-half and one-fourth of Htop, respectively, and group T-all consisted of all trees. Though the stands were man made, tree size varied greatly in many stands, and in some stands, the distribution of DBH was L-shaped as it is in natural forests. Since this study excluded the influence of undergrowth or stand structure on spectra to evaluate seasonal differences clearly, relatively homogeneous stands, in which more than 70% of the trees were in group T2, were selected for the analysis.

The average height of T1 (top layer height, H1) and stem volume/ha (Vha) were computed for each plot. The two parameters showed the highest correlation with the CASI data among the stand parameters such as average DBH, average height, and volume of each group in a preliminary analysis. H1 was related to the canopy size, and hence, to the surface roughness of the stands, while Vha was the total woody biomass, or the sum of the three-dimensional biomass concentration in the stands. This suggests that there are some differences in the relationships between these parameters and DN caused by the surface roughness and the biomass concentration. Although H1 showed a very strong positive correlation with Vha (Fig. 2), both H1 and Vha were analyzed separately to understand how DN was differently affected by the surface roughness and the biomass concentration, and how much the accuracy of the estimations of H1 and Vha differed.

Table 1 CASI data specification.

Observation date	Sep. 2, 1993	Oct. 3, 1994	Jun. 12, 1995
Observation time	10:35	10:00	10:08
Nominal flight height		3000 m	
Flight direction	325°	325°	330°
Solar azimuthal angle	153.7°	150.6°	131.3°
Solar zenith angle	37.1°	50.5°	26.5°
Field of view	35°	35°	42°
Nominal resolution		about 3.7 m × 3.7 m	
Pixel spacing cross truck	3.6 m	3.6 m	4.4 m
along truck	4.3 m	3.4 m	3.9 m
Quantization levels		12 bit (4096 levels)	
Spectral resolution		about 28 nm	
Observation channels* (nm)	446, 476, 507, 537, 567, 596, 626, 656, 687, 716, 746, 776, 806, 837, 867, 902**		

* The center wavelength in 1995. The center positions were different by about a few nanometers in 1993 and 1994. ** not observed in 1993.

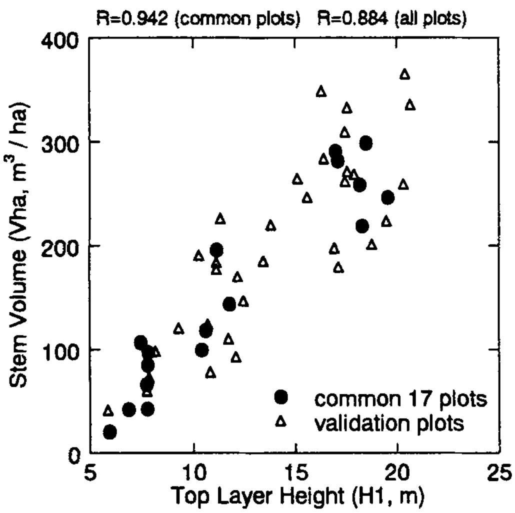

Fig. 2 Relationship between the top layer height (H1) and stem volume/ha (Vha) in all plots.

2 Selection of plot areas in the images

Since the skew corrections did not give accurate results, neither geometric correction nor co-registration of images was accurate. For this reason, plot locations were identified on all images by comparison with each other and by reference to plot locations on the color aerial photos. Fifty one training areas of the plots were selected carefully to choose the same areas in all images. The size of these training areas was between 40 and 60 pixels, which was large enough to cover the plots, and was different in each image due to differences of actual pixel spacing (Table 1). Then, the average, minimum and maximum DN of each channel were computed for each plot. Because of cloud cover and because the images covered different areas, the three images contained the same 17 plots (common plots), which were measured in 1993, 1994, and 1995 and one of them was a Todo fir stand. The September, October and June images contained 16, 16, and 20 other plots of the 51 plots, respectively. The common 17 plots were used for the correlation and regression analyses, and the other plots were used for accuracy validation (validation plots). Annual changes in forests, such as growth and thinning, were neglected in the analysis.

3 Analysis

Any significant difference in the spectra among the three evergreen conifers would affect the stand parameter estimation. Thus it was important to understand the spectral differences for the main species. However, forest spectra are influenced by not only species but also LAI, stand density, tree size, shadow of canopy, viewing angles of sensors, *etc.* (Kleman, 1987; Strahler *et al.*, 1988; Nilson and Peterson, 1994; Ranson *et al.*, 1994). Therefore, dense stands about 30 years old were selected as sample areas for the spectra comparison. There were not many uniform stands without invading broad-leaved trees in the images, and all species were found only in the October image. A one-way fractional analysis of variance (ANOVA) was applied to check the differences among tree species in the average DN in each channel, while multiple comparison tests (the Scheffé's tests) were applied to examine the differences in the average DN between and within species.

Relationships between the average, minimum and maximum DN and the stand parameters of the 17 plots were analyzed as follows. (1) The relationships between DN and H1, and DN and Vha were examined using scattergrams. (2) The correlation coefficients between DN and H1, and DN and Vha were calculated. The correlation coefficients between logarithm of DN and the stand parameters were also calculated. The best wavelength channel and image (season) were evaluated by correlograms. The influence of the fraction of deciduous broad-leaved trees, which were calculated by the number of stems, was also examined by correlation coefficients. (3) Linear regression models were developed for some combinations with higher correlation coefficients. Accuracy of the estimates obtained from the regression models was judged using the validation plots. (4) Spatial patterns of the stand parameters were examined visually. Furthermore, the differences among the three images were analyzed. (5) The best season among the three was evaluated to summarize the results.

The spatial pattern was derived as follows. First, the images were geo-referenced to make comparison easier. Ground control points (GCPs) were selected using digitized forest planning maps. Although the geometric accuracy was not sufficient, second-order polynomials were computed with the GCPs because higher order polynomials did not improve the accuracy. The nearest neighbor method was adopted for resampling, and the mesh size was set to 3.5 m to avoid losing pixels. Secondly, filtering was applied to the images. The linear regression models were also applied to the local minimum and average DN within areas that were similar to the plots, since the minimums and averages were used in the regression analysis. A circular moving window with a diameter of 7 pixels was employed as kernels for the minimum and low pass filtering. As a consequence, the minimum filter passed the minimum DN within the moving window, and the low pass filter averaged pixel values within the moving window as well. The minimum and low-pass filters were applied to the geo-referenced images to produce the local minimum and the local average images respectively. Finally, the spatial distributions of H1 and Vha were obtained from the linear regression models, and the local minimum and the local average images respectively.

The spatial patterns of H1 and Vha were evaluated as follows. The evergreen conifer areas were extracted visually for prints (Fig. 8) by comparing the images with the forest planning maps. The estimation results were compared with each other visually. Sixteen areas, which were located near the nadir in all images, were selected with tree size differences being considered (comparison areas). The areas each consisted of approximately 150 pixels. The average of H1 and Vall were calculated for all results. Relationships among the three seasons were analyzed by a linear regression analysis.

Results and Discussion

1 Spectra of spruce and fir

Differences between and among spectra of one Ezo spruce, two Akaezo spruce and three Todo fir stands were examined for the October image. The spectra with the closest resemblance among the three species are shown in Fig. 3. Although Todo fir seemed to have higher DN in the NIR channels between 746 and 902 nm than the two spruce species, the spectra were very similar visually. According to the ANOVA, the average DNs of the six stands were significantly different at the 0.01 level in all channels. The multiple comparison tests showed significant differences at the 0.01 level in the average DNs for all combinations of the six stands in three or more channels, even within the same species. There were three major factors considered causing these spectral differences, which were directional reflectance characteristics (Kleman, 1987; Ranson *et al.*, 1994), species and stand conditions including the stand parameters. However, the directional reflectance characteristics were minimal because the flight direction and the solar principal plane were nearly parallel for the October image. Spectral variations not only among species but also within species seemed large. This suggested that the factors such as tree size and stand density had strong influences on forest spectra, and it was very difficult to determine the spectral differences among those three species. Since spectral differences among evergreen conifers are smaller in autumn than in summer (Awaya and Tanaka, 1999), there was possibly a larger spectral variation in the other images. Spectral differences among these three species were not included in the following discussion.

2 Relationship between DN and stand parameters

A negative correlation was observed in most combinations of DN and the stand parameters. Three examples of scatter-

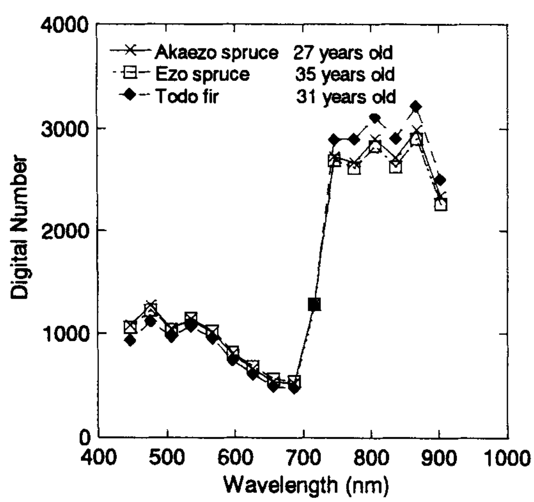

Fig. 3 Spectra of Akaezo spruce, Ezo spruce, and Todo fir in the CASI image of October 3, 1994. Spectra from dense stands about 30 years old are selected. Although the spectra appear similar, the ANOVA showed significant difference in the average DN among stands at the 0.01 level in all channels for the 6 stands. The differences between the averages were significant at the 0.01 level in any stand combinations in three or more channels according to the results of a multiple comparison test.

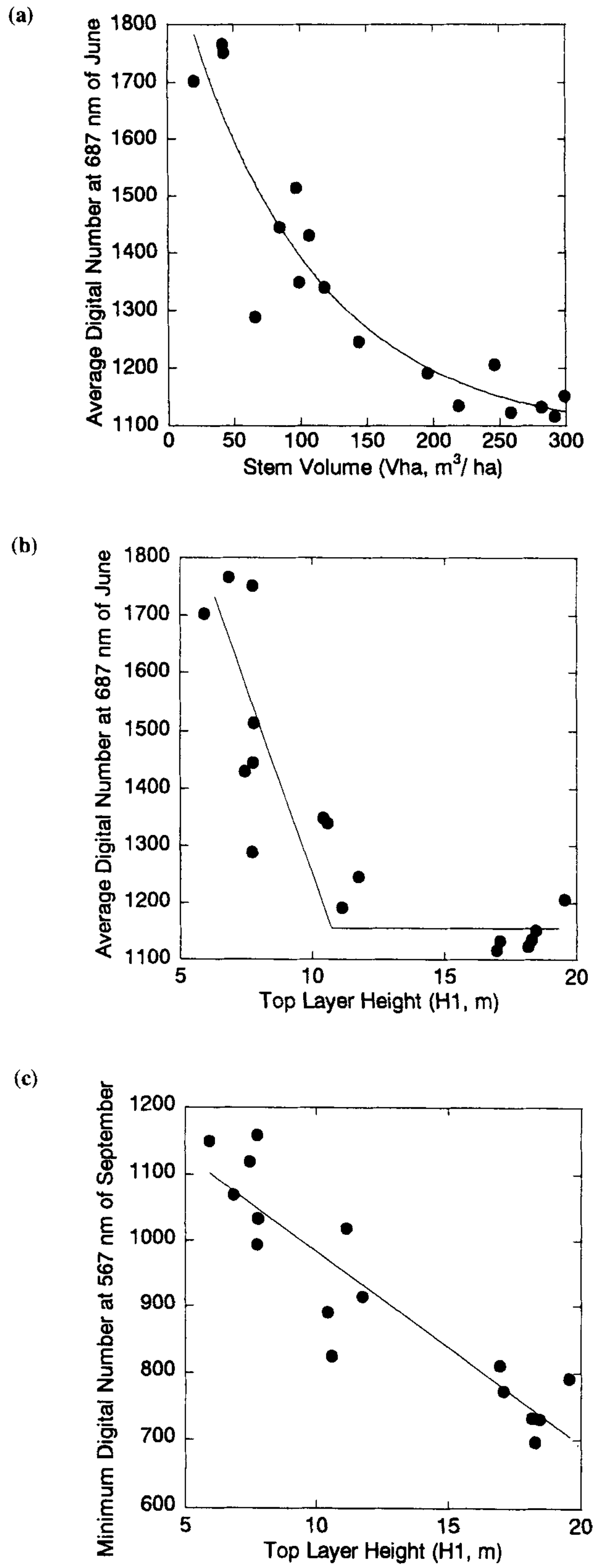

Fig. 4 Three typical patterns of scattergrams between DN and the stand parameters. a) a curvilinear case between the stem volume/ha (Vha) and the average DN at 687 nm in 1995, b) a linear case with an inflection point between the top layer height (H1) and the average DN at 686 nm in 1995, and c) a linear case between H1 and the minimum DN at 567 nm in 1993.

grams are shown in Fig. 4. Negative relationships are common between the stand parameters (LAI, DBH, tree height, woody volume and so on) and DN (or radiance, or reflectance factor) in visible and NIR channels (Franklin, 1986; Peterson *et al.*, 1987; Spanner *et al.*, 1990; Franklin and McDermid, 1993; Baulies and Pons, 1995). Reflectance of vegetation (overstory) and soil (background) regulates the relationship between reflectance and LAI for crops according to a radiative transfer model (Sellers, 1987). Therefore, upper trees and undergrowth would influence the stand parameter estimation in forests.

The scattergrams were classified into three patterns. The curvilinear relationship (Fig. 4a) was most likely to appear (Franklin, 1986; Peterson *et al.*, 1987; Spanner *et al.*, 1990; Cohen and Spies, 1992). Two lines with an inflection point (Fig. 4b) were a variation of the curvilinear pattern. A part of these two relationships was the linear relationship (Fig. 4c). Relationships between Vha and DN were near linear for most channels, while H1 and DN showed linear and curvilinear relationships for the green (around 550 nm) and the NIR channels (between 776 and 902 nm), respectively, and the blue channels (around 445 nm) did not show a clear tendency. The intensity of the Rayleigh scattering is proportional to the inverse fourth power of wavelength (Silva, 1978), but the reflectance factor of green trees is very small in the blue region (approximately 1–2%, Williams, 1991). Different viewing geometry may result in large variations in the scattering in different parts of images. These variations disturbed the DN-parameter relationship in the blue region.

Gemmell (1995) reported near linear relationships for a conifer forest between DN and timber volumes from 80 to 250 m^3/ha in plots in the red and NIR channels using TM images. However, the numerical simulation showed a curvilinear relation, when volume exceeded 300 m^3/ha (Gemmell, 1995). Vha ranged between 20 and 300 m^3/ha for the case of 17 common plots in this study (Fig. 2), and the relations between the average DN and Vha were near linear using the green and red channels. Near linear relationships were also obtained for the NIR channels except for the NIR channels of the June image. These results were similar to those of Gemmell (1995). Thus, linear models were reasonable for this study, and a curvilinear model would be necessary, if Vha exceeds 300 m^3/ha.

3 Correlation coefficients

1) Difference in minimum, average and maximum DN and channels

The correlation coefficients between H1 and the minimum DN (r_{min}), the average DN (r_{ave}) and the maximum DN (r_{max}) at 567 nm were in the order $r_{min} > r_{ave} > r_{max}$, (Table 2). The minimum DN contained larger shadow parts of canopies than the average and the maximum DN, and the undergrowth had little influence in the minimum DN due to the shadows. Upper trees of evergreen conifers and shadows were the major components within all pixels of the minimum DN. Thus, the shadow ratio within the pixel was changed according to the upper tree size, and caused the linear relationship in 567 nm for H1. Since the minimum DN was one of the textural attributes, this confirmed the importance of texture for the stand parameter studies as reported previously (Cohen *et al.*, 1990; Cohen and Spies, 1992; Flanklin and McDermid, 1993; St-Onge and Cavayas, 1997). If the ground resolution of CASI data was finer, an asymptotic value, which was DN of pixels containing only shadows of canopies, would exist. This suggested that there are different appropriate ground resolutions for different forest types for tree height estimation. However, there was a risk that the minimum DN could be affected by the noise of sensors.

On the other hand, there was not a clear tendency in the intensity order of correlation coefficients for Vha (Table 2) against the minimum, the average and the maximum DN at 806 nm in the three images. Broad-leaved trees would affect the maximum and probably the average DN, because spectra using the maximum DN resembled those of broad-leaved trees in some stands. This means that the mixture of broad-leaved trees affected the stand parameter estimation. Vha may have the highest correlation with the average DN in some channels due to the effects of biomass on DN, even if the mix-

Table 2 Correlation coefficients between H1, Vha, and CASI data.

H1		Original CASI data			Logarithm of CASI data		
Image	Wavelength	Average	Maximum	Minimum	Average	Maximum	Minimum
Sep. '93	567 nm	− 0.892**	− 0.769**	− 0.917**	− 0.906**	− 0.778**	− 0.929**
Sep. '93	806 nm	− 0.705**	− 0.711**	− 0.810**	− 0.758**	− 0.753**	− 0.857**
Oct. '94	567 nm	− 0.883**	− 0.880**	− 0.915**	− 0.900**	− 0.881**	− 0.923**
Oct. '94	806 nm	− 0.815**	− 0.835**	− 0.788**	− 0.848**	− 0.846**	− 0.798**
Jun. '95	567 nm	− 0.761**	− 0.634**	− 0.789**	− 0.777**	− 0.647**	− 0.792**
Jun. '95	806 nm	− 0.169	− 0.121	− 0.424	− 0.113	− 0.082	− 0.403
Vha							
Sep. '93	567 nm	− 0.894**	− 0.756**	− 0.860**	− 0.903**	− 0.758**	− 0.861**
Sep. '93	806 nm	− 0.780**	− 0.781**	− 0.844**	− 0.821**	− 0.813**	− 0.867**
Oct. '94	567 nm	− 0.903**	− 0.923**	− 0.841**	− 0.916**	− 0.923**	− 0.843**
Oct. '94	806 nm	− 0.864**	− 0.864**	− 0.768**	− 0.890**	− 0.873**	− 0.753**
Jun. '95	567 nm	− 0.836**	− 0.708**	− 0.739**	− 0.850**	− 0.792**	− 0.783**
Jun. '95	806 nm	− 0.336	− 0.325	− 0.517	− 0.283	− 0.286	− 0.493*

The correlation coefficients are significant at the 0.05 level (*) and at the 0.01 level (**).

ture of broad-leaved trees is also affected.

Since absorption of tree leaves is strong in the visible region, light scarcely penetrates the leaf layers (Awaya *et al.*, 1999). Therefore, DN mainly provided information on the canopy surfaces in the visible region, and the surface information appeared in H1. Meanwhile, high transmittance allowed light to penetrate the leaf layers in the NIR region (Awaya *et al.*, 1999), and DN was influenced by trees in not only the upper layers but also the under story. Variations of reflectance factors among trees and among species (Awaya and Tanaka, 1999) appeared to be greater in the NIR than in the visible regions, thus affecting the relationship between the stand parameters and DN in the NIR region. This can be explained as the cause of the differences in H1 and Vha in the relationship at 567 nm and 806 nm in Table 2.

2) Difference in seasons and channels

The visible channels gave higher correlation coefficients than the NIR channels (Fig. 5). The highest correlation was observed in the green channels at 567 and 596 nm in September and October, although in the red channels, it was observed at 656 and 687 nm in June. In the visible and NIR regions, the red region seems to give higher correlations with the stand parameters (Peterson *et al.*, 1987; Spanner *et al.*, 1990; Franklin and McDermid, 1993). However, the green region gives almost the same correlation coefficients as the red region (Franklin, 1986), while the NIR region presents a poor correlation in some cases (Franklin, 1986; Peterson *et al.*, 1987; Spanner *et al.*, 1990), but higher correlation in others (Baulies and Pons, 1995; Trotter *et al.*, 1997). In fact, our results agreed with the above statements. Namely, the red channels presented consistently good results, and the green channels presented the best results in some seasons. The NIR channels manifested obvious large seasonal variations in correlation coefficients with the stand parameters.

Correlation coefficients were higher in September and October than in June in the green (around 567 nm) and NIR

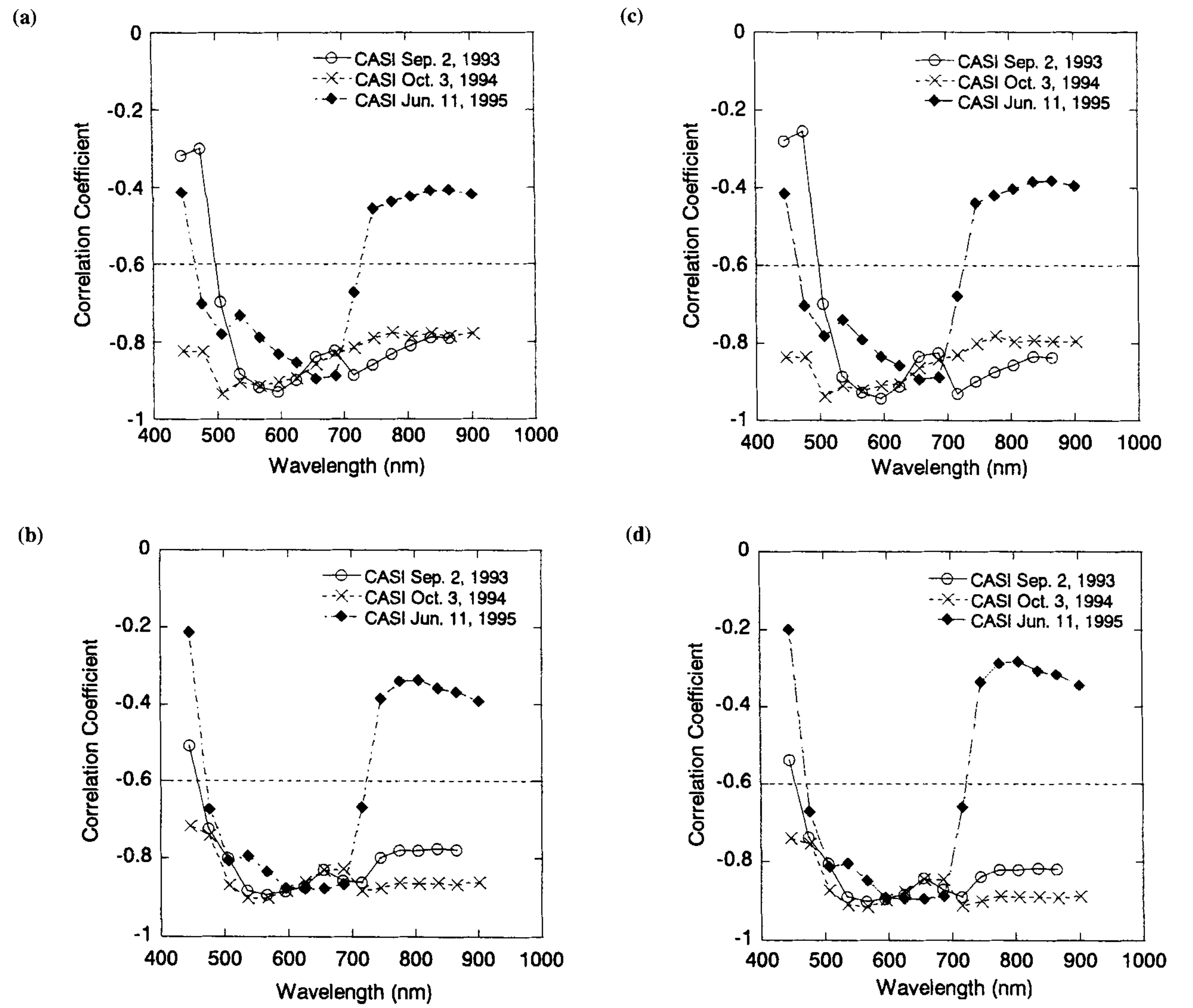

Fig. 5 Correlograms between DN and the stand parameters. a) between the minimum DN at 567 nm for September and October, at 656 nm for June and the top layer height (H1), b) between the average DN at 567 nm for September and October, at 656 nm for June and the stem volume/ha (Vha), c) between the natural logarithm of the minimum DN at 567 nm for September and October, at 656 nm for June and H1, and b) between the natural logarithm of the average DN at 567 nm for September and October, at 656 nm for June and Vha. The correlation coefficients below the dashed straight lines are significant at the 0.01 level.

(between 776 and 902 nm) channels (Fig. 5). Trees grew fresh leaves from late May through June, and trees may have leaves in different physiological conditions at the time. Since leaves change their spectra greatly during the leaf maturation process (Howard, 1991), there were spectral variations among trees in the June image. Reflectance changes considerably in the NIR, but hardly in the blue and red regions (Howard, 1991), which indicates that trees had more similar reflectance to each other in the blue and red channels than in the other channels in the June image.

Tree canopies have higher reflectance factors in the green than red regions although the difference is not significant (Williams, 1991). Extremely strong absorption of evergreen conifers may obscure the surface information in the red channels in September and October, and stronger reflectance factors may provide greater surface information in the green channels. On the other hand, spectral variation by fresh leaves in the green channels would affect the data in June, and the red channels were better than the green channels for the stand parameter studies in June. The spectral variation reduced correlation coefficients for most channels in June (Fig. 5).

Since some channels had a curvilinear relationship with H1 and Vha, the logarithm of DN was compared with the original DN on the relationships with the stand parameters. Correlation coefficients were improved in the red edge at 716 and 746 nm and NIR regions of the September image against H1 and of all images against Vha when the logarithm of DN was taken (Fig. 5c, d). There was little improvement in the visible regions due to the near linear relationship between the original DN and the stand parameters. Therefore, it was unnecessary to develop curvilinear models for the combinations of visible channels and these two parameters in this case.

According to some previous studies of this field, the most accurate estimation is possible for homogenous evergreen conifers with the coefficients of determination of 0.89 by a log-linear model (Peterson *et al.*, 1987), 0.51 by a log-linear model (Spanner *et al.*, 1990) for LAI, and 0.56 by a linear model for DBH (Flanklin and McDermid, 1993). Estimation accuracy is lower in complex species composition -0.29 by a log-linear model for the basal area (Franklin, 1986), and 0.36 by a linear model for canopy closure in a mountainous terrain (Baulies and Pons, 1995). These results were derived for the red region except for the result of Baulies and Pons (1995), which was for the NIR region. The plot data of this study were of dense evergreen conifer stands in flat terrains, which meant that there were not many broad-leaved trees to cause high reflectance and affect DN in conifer stands, and the topography and undergrowth had little effect on DN. Although uneven topography, undergrowth and broad-leaved trees degraded the accuracy of the stand parameter estimation, their effects were minimal in this study. Thus the results of this study were obtained from nearly ideal cases and with the number of plots being only 17, high coefficients of determination were therefore observed.

3) Influence of deciduous broad-leaved trees

The correlation coefficients between DN and the fraction of broad-leaved trees were verified. The highest correlation coefficients were 0.333, 0.449, and 0.433 respectively for the minimum DN at 596 nm in September, the maximum DN at 746 nm in October and the minimum DN at 567 nm in June. The correlation coefficients were positive for most channels, and none of them was significant at the 0.05 level. On the contrary, the correlation coefficients for H1 and Vha were significant at the 0.01 level in most channels (Fig. 5 a, b). This suggested that even though there was a significant negative correlation ($r = -0.490$) between the fraction of broad-leaved trees and H1 at the 0.05 level, the stand parameters were more influential on DN than the fraction of broad-leaved trees.

4 Estimation of stand parameters

1) Validation

Linear models were developed for the green channel (567 nm) in the September and October images and for the red channel (656 nm) in the June image for H1 and Vha with the 17-plot data (Fig. 6). Curvilinear models were also developed for the same combinations of linear models. By examining the results with the validation plot data, the linear models showed constant residuals between the measured and estimated stand parameters especially for H1 (Fig. 7), while the curvilinear models showed outliers in the validation results. This may not always be the case; however, the results implied the difficulty of applying curvilinear models. To obtain consistent accuracy, it was more sensible to employ channels and the stand parameters which showed a linear relationship.

In the linear models, Vha was underestimated in higher volumes, but H1 corresponded considerably well with the measured one in the range of validation plots. The difference may be related to the characteristics of H1 and Vha, the surface roughness and the three dimensional biomass concentration, respectively. H1 was a better parameter than Vha for achieving finer accuracy in our results. However, only half of the validation plots were included in the line, which crosses the origin with the slope of 1, within their confidence intervals at the 0.95 level even for the best result (the linear model between H1 and the minimum DN at 567 nm in September). This result may barely be acceptable for practical uses, and further validation is necessary.

2) Spatial patterns

As regards the spatial distribution, both H1 and Vha were underestimated in the northeastern edges of the September and October images, and overestimated in the northeastern edge of the June image (Fig. 8). Since common plots were needed for the model development, the southwestern half of the June image was selected here. Being the sunny side (back scattering side) of the canopy, DN in this part was larger than on the shade side (forward scattering side) in the northeastern half. The equations were adjusted to the sunny side, and they resulted in overestimates on the shade side. On the contrary, the common plots were located near the nadir in the September and October images, and the stand parameters

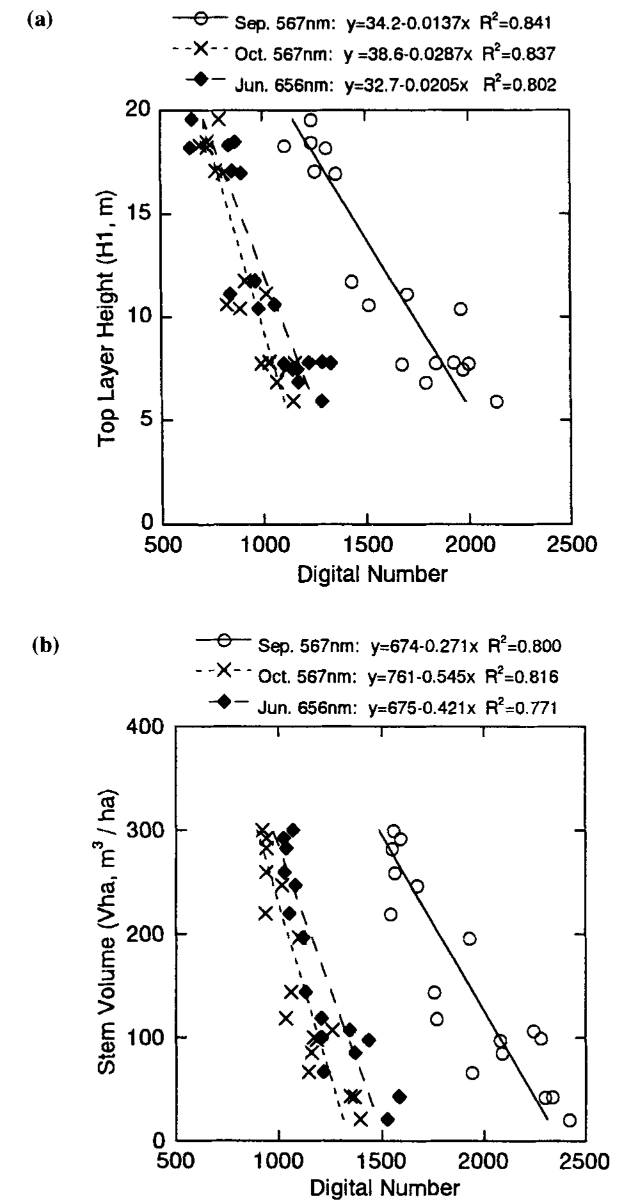

Fig. 6 Scattergrams between DN and the stand parameters with regression lines for spatial estimation. a) between the minimum DN at 567 nm for September and October, at 656 nm for June and the top layer height (H1), and b) between the average DN at 567 nm for September and October, at 656 nm for June and the stem volume/ha (Vha). The equations were used to estimate those parameters using CASI images. The slope coefficients of the three equations are significant at the 0.01 level.

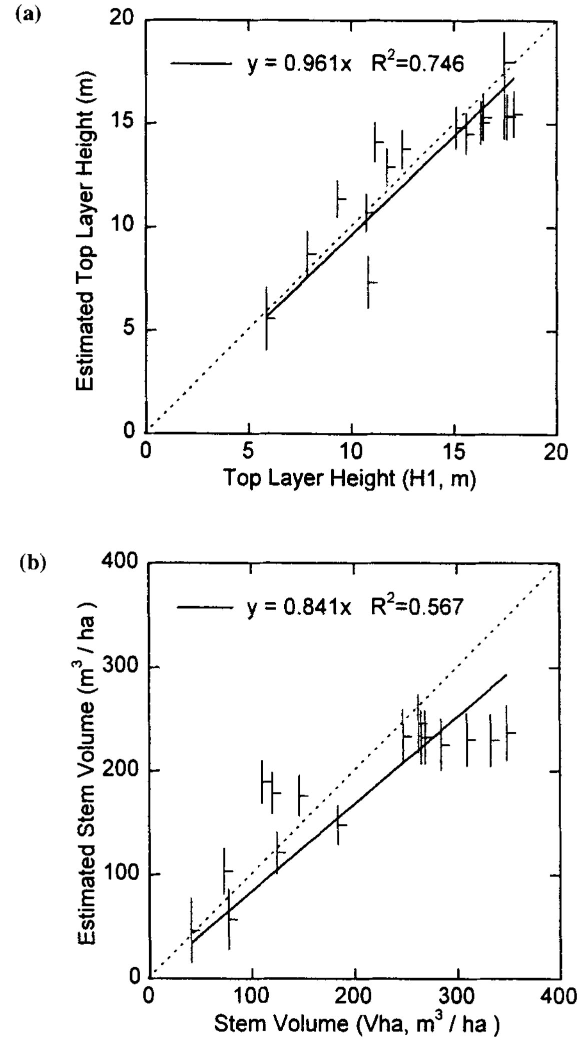

Fig. 7 Scattergram between the measured and estimated stand parameters. a) The relationship for the case of the top layer height (H1) using the minimum DN and the September image, and b) the relationship for the case of the stem volume/ha (Vha) using the average DN and the September image. H1 has a near one-to-one relationship between the measured and the estimated H1, but Vha may be saturated over 280 m^3. The vertical lines show the confidence intervals at the 0.95 level. The slope coefficients of the two equations are significant at the 0.01 level.

were underestimated in the eastern edges. Although the flight direction and the solar azimuthal angle were nearly parallel for each image even for the June image (Table 1), the strong directional reflectance properties of the evergreen conifers in the visible region (Kleman, 1987; Ranson *et al.*, 1994) may have caused a bias. This suggested that wide or off-nadir viewing images cause serious bias on the stand parameter estimations, especially when training samples are selected from a part of the images. For this reason, narrower viewing sensors such as TM, of which FOV is 15.4 degrees, are favorable for the stand parameter studies. Spatial patterns except those on the northeastern side (right side in Fig. 8) appeared similar to each other, provided that the results were reasonable and compatible, although the parameters were overestimated at the edge of stands and along forest roads.

The results were almost equal to each other (Fig. 9). The September results were in the middle among the three seasons both for H1 and Vall. Vall showed a slightly greater variation than H1 compared with the September results. As for Vall, it was about 6% overestimated in June, and about 7% underestimated in October especially in young stands compared with that in September. As regarding H1, it was about 6% underestimated in October, and was almost the same in June compared with that in September. The coefficients of determination of linear equations between them were prominent, and the

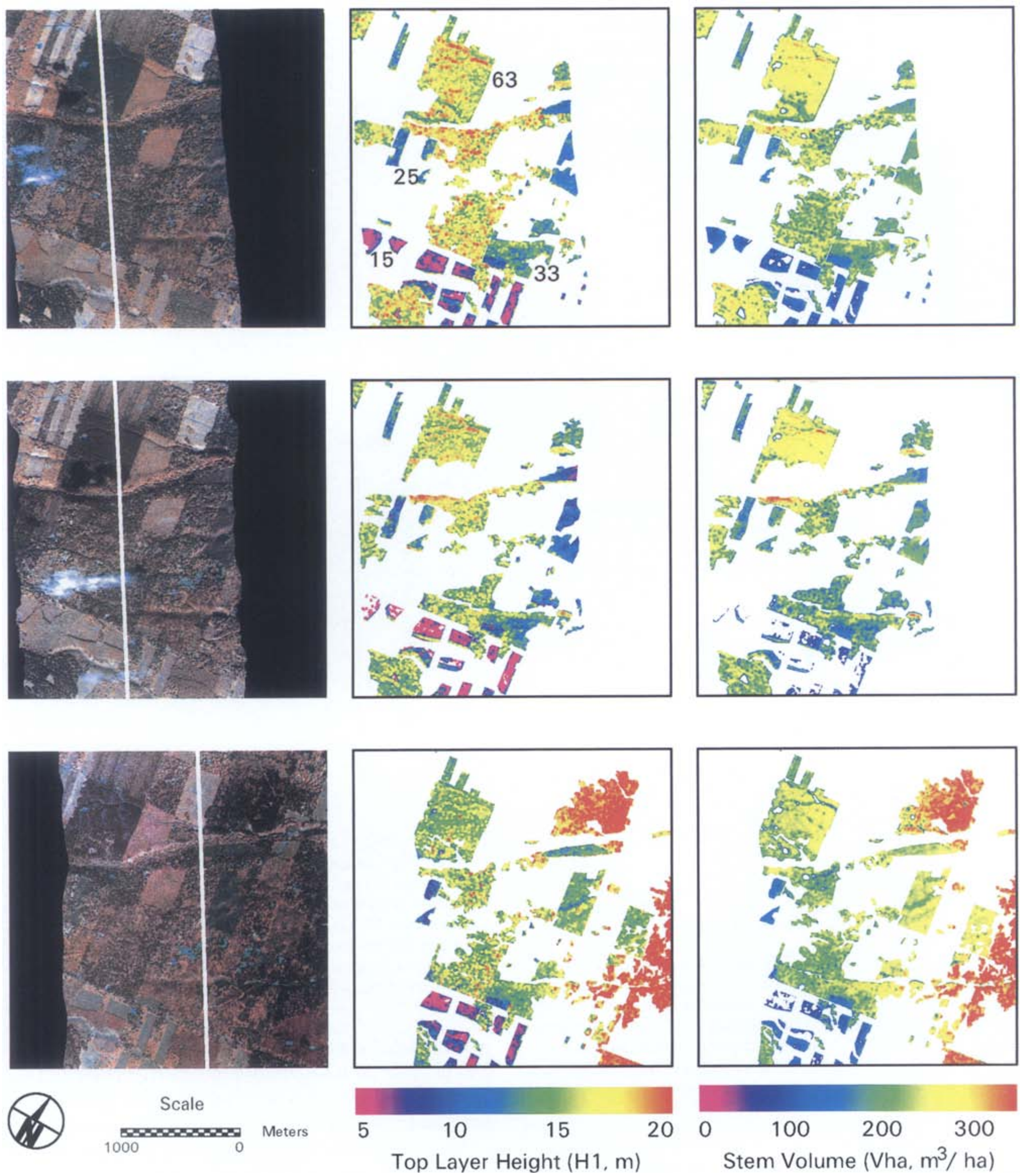

Fig. 8 Spatial distribution of the estimated parameters. left: CASI images (R: 7 ch, B: 3ch, R15ch), middle: H1, right: Vha, upper: September 1993, middle: October 1994, and bottom: June 1995. The top layer height (H1) and the stem volume/ha (Vha) are overestimated at the right half of the June image. However, spatial patterns are similar among three results in the left half of the June image and other images. The white lines are the flight centers. Evergreen stands are delineated visually by judging using forest planning maps and CASI images. Numbers in the upper middle are stand age in 1993.

results were nearly identical, though autumnal colors and defoliation may have affected the October cases and caused an underestimation.

5 Best season for stand parameter estimation

As discussed above, leaf maturation affected the spectra in the early growing season. The reflectance factors exceeded the

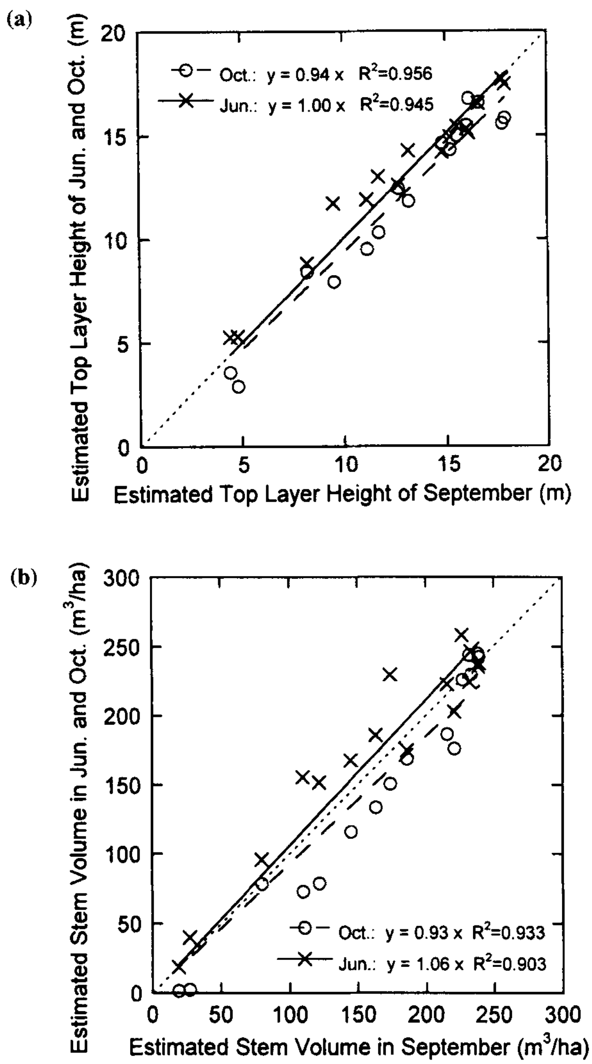

Fig. 9 Relationships between the estimated stand parameters between images. a) the case of top layer height (H1) between the September and October images, the September and June images, and b) the case of stem volume/ha (Vha) between the September and October images, the September and June images. The slope coefficients of the four equations are significant at the 0.01 level.

maximum in early July and dropped remarkably in early August in the NIR regions in Tomakomai (Awaya and Tanaka, 1999), and then the effects of leaf maturation decreased after August. As the correlograms showed higher correlation coefficients in all channels in the late growing season than early growing season except for the two red channels (Fig. 5), the late growing season was a proper time for obtaining images. However, autumnal coloring was recognized in the October image, and deciduous trees had higher reflectance factors than evergreen trees in the visible and NIR regions during the growing season (Awaya and Tanaka, 1999). It is possible to avoid or reduce the effects of broad-leaved trees in conifer stands, when pixels of only evergreen conifers are selected by image processing. The minimum filtering would select only dark pixels of either conifer trees or shadows. If the fraction of broad-leaved trees is less than that of conifer trees, the median filtering would select conifer pixels, since the median is DN of a conifer pixel in this case. Thus it is satisfactory to reduce the effects of broad-leaved trees by the filtering.

Conclusions

The objectives of this study were, firstly, to analyze the relationships between the DN of three CASI images and the stand parameters—the top layer height (H1) and the stem volume/ha (Vha); secondly, to evaluate favorable channels and seasons for the parameter estimations; and thirdly, to examine the estimation accuracy of H1 and Vha. The conclusions were drawn as follows:

(1) The DN was influenced by the stand conditions such as species composition, tree density and undergrowth, and consequently the stand conditions affected the accuracy of the stand parameter estimation. Our results suggested that the spatial estimation of the stand parameters, especially H1, was reliable with sufficient accuracy in the case of dense evergreen conifer stands in flat terrain. Nadir viewing images were necessary to achieve sufficient accuracy.

(2) There were three basic patterns (curvilinear, linear with an inflection point and linear) in the scattergrams between the stand parameters and DN. Negative relationships were most common between them in all channels.

(3) The minimum DN had the highest correlation with H1, indicating that the texture of canopies has a strong influence as stated previously. The canopy texture appeared in the CASI images due to their high spatial resolution.

(4) The red channels showed high correlation coefficients with H1 and Vha consistently for the three images, and the red channels were reliable in all seasons for H1 and Vha estimation.

(5) On the other hand, the highest correlation coefficients were obtained with the green region in the September and October images, and high correlation was discovered even with the NIR region in these images. The spectral variation among trees in June probably disturbed the DN and the stand parameter relationships. Therefore images in the late growing season yielded high accuracy.

Since evergreen conifers, except for pines, had similar spectral characteristics in our experiences, similar results were likely to be derived in other species. However, as radiometric bias by topography was a critical problem in the utilization of remote sensing in mountainous regions, it was necessary for it to be corrected to allow wider application of the present results.

The authors would like to express their heartfelt gratitude to Dr. Takashi Moriyama (NASDA) and Mr. Hiroshi Oguma (National Institute of Environmental Studies, previously NASDA) for their support of the airborne and field surveys. They are also thankful to Dr. Mitsuo Inose (Forestry and Forest Products Research Institute, FFPRI), Dr. Norihiko Shiraishi (The Univ. of Tokyo), Dr. Satoshi Ishibashi (FFPRI), Dr. Makoto Sano (FFPRI), Dr. Nobuyuki Abe (Niigata Univ.), Dr. Masato Katoh (Hokkaido Forestry Institute), Anssi Lohi (Technical Research Center of Finland) and many other people who have helped in the forest surveys. They also thank Dr. Shiraishi for providing the software for estimating the tree height curve as well. Finally, special thanks are given to NASDA for executing this study jointly with the authors and for providing the CASI images.

This study was also partly supported by the research project, 'A Study of Accurate Biomass Estimation using Airborne Imagery,' of the Science and Technology Agency of Japan. Comments from the editors helped improve the contents of the paper. The authors are grateful for their kind cooperation and valuable advice.

Literature cited

Awaya, Y. and Tanaka, N. (1999) Seasonal spectral changes in cool temperate forests: An Analysis using Landsat TM data. Jpn. J. Photogram. Remote Sens. 38 (4): 35–46. (in Japanese with English summary)

Awaya, Y., Miller, J.R., and Freematle, J.R. (1992) Background effects on reflectance and derivatives in an open-canopy forest using airborne imaging spectrometer data. *In* International Archives of Photogrammetry and Remote Sensing, XXIX B7. ISPRS, Washington, D.C., 836–843.

Awaya, Y., Tanaka, K., Sawada, H., and Takao, G. (1999) Seasonal changes of transmittance spectra in a beech stand: Measurement method and outline of seasonal changes. Tohoku J. Forest Sci. 4–1: 1–7. (in Japanese with English summary)

Babey, S.K. and Anger, C.D. (1989) A Compact Airborne Spectrographic Imager (CASI). *In* Proceedings of International Geoscience and Remote Sensing Symposium, (IGARSS '89). Vol. 12, IGARSS, Vancouver, 1028–1031.

Baulies, X. and Pons, X. (1995) Approach to forestry inventory and mapping by means of multi-spectral airborne data. Int. J. Remote Sens. 16: 61–80.

Blackburn, G.A. and Milton E.J. (1995) Seasonal variations in the spectral reflectance of deciduous tree canopies. Int. J. Remote Sens. 16: 709–720.

Chen, J.M. and Cihlar, J. (1996) Retrieving leaf area index of boreal conifer forests using Landsat TM images. Remote Sens. Environ. 55: 153–162.

Cohen, W.B. and Spies, T.A. (1992) Estimating structural attributes of Douglas-fir/western hemlock forest stands from Landsat and SPOT imagery. Remote Sens. Environ. 41: 1–17.

Cohen, W.B., Spies, T.A., and Bradshow, G.A. (1990) Semivariograms of digital imagery for analysis of conifer canopy structure. Remote Sens. Environ. 34: 167–178.

Cohen, W.B., Spies, T.A., and Fiorella, M. (1995) Estimating the age and structure of forests in a multi-ownership landscape of western Oregon, USA. Int. J. Remote Sens. 16: 721–746.

Curran, P.J. (1983) Multispectral remote sensing for the estimation of green leaf are index. Phil. Trans. R. Soc. Lond. A. 309: 257–270.

Curran, P.J., Dungan, J.L., and Gholz, H.L. (1990) Seasonal LAI in Slash pine estimated with Landsat TM. 19pp, NASA TM-102278, Ames Research Center, National Aeronautics and Space Administration, Moffett Field, California.

Franklin, J. (1986) Thematic Mapper analysis of coniferous forest structure and composition. Int. J. Remote Sens. 7: 1287–1301.

Franklin, S.E. and McDermid, G.J. (1993) Empirical relations between digital SPOT HRV and CASI spectral response and lodgepole pine (*Pinus contorta*) foerst stand parameters. Int. J. Remote Sens. 14: 2331–2384.

Gemmell, F.M. (1995) Effects of forest cover, terrain, and scale on timber volume estimation with Thematic Mapper data in a Rocky Mountain site. Remote Sens. Environ. 51: 291–305.

Hokkaido Forestry Bureau (1970) Standing tree volume table. 50pp, Rinya Kohsaikai, Sapporo. (in Japanese)*

Holben, B.N., Tucker, C.J., and Fan, C. (1980) Spectral assessment of soybean leaf area and leaf biomass. Photogramm. Eng. Remote Sens. 46: 651–656.

Howard, J.A. (1991) Remote sensing of forest resources. 420pp, Chapman and Hall, London.

Huete, A.R. (1987) Soil influences in remotely sensed vegetation-canopy spectra. *In* Theory and applications of optical remote sensing. Asrar, G. (ed.), 734pp, John Willey and Sons, New York, 107–141.

Kleman, J. (1987) Directional reflectance factor distributions for two forest canopies. Remote Sens. Environ. 23: 83–96.

Leprieur, C.E., Durand, J.M., and Peyron, J.L. (1988) Influence of topography on forest reflectance using Landsat Thematic Mapper and digital terrain data. Photogramm. Eng. Remote Sens. 54: 491–496.

Nakashima, H. (1946) Standing volume table for some forest types and areas of Hokkaido. Hokkaido Branch of Kohrinkai, 4. (in Japanese)*

Nilson, T. and Peterson, U. (1994) Age dependence of forest reflectance: analysis of main driving factors. Remote Sens. Environ. 48: 319–331.

Peterson, D.L., Spanner, M.A., Running, S.W., and Teuber, K.B. (1987) Relationship of Thematic Mapper simulator data to leaf area index of temperate coniferous forests. Remote Sens. Environ. 22: 323–341.

Ranson, K.J., Irons, J.R., and Williams, D.L. (1994) Multispectral bidirectional reflectance of nothern forest canopies with the Advanced Solid-State Array Spectroradiometer (ASAS). Remote Sens. Environ. 47: 276–289.

Sellers, P.J. (1987) Canopy reflectance, photosynthesis, and transpiration II. The role of biophysics in the linearity of their interdependence. Remote Sens. Environ. 21: 143–183.

Silva, L.F. (1978) Radiation and instrumentation in remote sensing. *In* Remote sensing: The quantitative approach, Swain, P.H. and Davis, S.M. (ed.), McGraw Hill, 330pp, New York, 35–36.

Spanner, M.A., Pierce, L.L., Peterson, D.L., and Running, S.W. (1990) Remote sensing of temperate coniferous forest leaf area index: The influence of canopy closure, understory vegetation and background reflectance. Int. J. Remote Sens. 11: 95–111.

St-Onge, B.A. and Cavayas, F. (1997) Automated forest structure mapping from high resolution imagery based on directional semivariogram estimates. Remote Sens. Environ. 61: 82–95.

Strahler, A.H., Wu, Y., and Franklin, J. (1988) Remote estimation of tree size and density from satellite imagery by inversion of a geometric-optical canopy model. *In* Proceedings of the 2nd International Symposium on Remote Sensing of Environment, Abidjan, Côte d'Ivoire, 337–348.

Tomakomai Forestry Office (1993) The 1st forest management plan of Tomakomai Forestry Office. 47pp, Hokkaido Forestry Bureau, Sapporo. (in Japanese)*

Trotter, C.M., Dymond, J.R., and Goulding, C.J (1997) Estimation of timber volume in a coniferous plantation forest using Landsat TM. Int. J. Remote Sens. 18: 2209–2223.

Williams, D.L. (1991) A comparison of spectral reflectance properties at the needle, branch, and canopy level for selected conifer species. Remote Sens. Environ. 35: 79–93.

* The English titles are tentative translations from the original Japanese titles by the authors of this paper.

(Accepted July 4, 2000)